Evidence of chemical bonding in the electronic structure of a metastable $Fe_{80}Cu_{20}$ alloy

2001 J. Phys.: Condens. Matter 13 5723

(http://iopscience.iop.org/0953-8984/13/24/317)

INSTITUTE OF PHYSICS PUBLISHING JOURNAL OF PHYSICS: CONDENSED MATTER

J. Phys.: Condens. Matter **13** (2001) 5723–5729 www.iop.org/Journals/cm PII: S0953-8984(01)23062-8

Evidence of chemical bonding in the electronic structure of a metastable $Fe_{80}Cu_{20}$ alloy

M Abbate[1], W H Schreiner[1], T A Grandi[2] and J C de Lima[2]

[1] Departamento de Física, UFPR, Caixa Postal 19091, 81531-990 Curitiba PR, Brazil
[2] Departamento de Física, UFSC, Caixa Postal 476, 88040-900 Florianopolis SC, Brazil

Received 19 March 2001, in final form 1 May 2001

Abstract

We studied the electronic structure of a metastable $Fe_{80}Cu_{20}$ alloy using x-ray photoelectron spectroscopy (XPS). The sample was produced by ball-milling, giving single-phase (BCC) nanoparticles with a diameter of about 10 nm. The core level Fe 2p and Cu 2p spectra of the alloy are rather similar to those of the individual Fe and Cu constituents; the absence of chemical shifts in these spectra indicates that the charge transfer between the Fe and Cu is negligible. On the other hand, the valence band spectrum of the alloy deviates from a linear combination of the corresponding Fe and Cu bands. The difference in the valence band of the alloy is attributed to bonding interactions between the Fe 3d and Cu 3d states. This illustrates the presence of chemical bonding between the valence electrons in a metastable alloy made of immiscible elements.

1. Introduction

Mechanical alloying has been used for almost two decades to produce many unique materials. These include, for instance, nanocrystalline alloys, amorphous compounds and metastable phases. The starting point of the mechanical alloying technique is a blend of crystalline elemental powders. Upon initial milling, there is a fast reduction in the particle size of the mixture of the elemental components. The elemental powder particles are then cold welded by the colliding balls resulting in composite particles. Further milling leads to nanometre sized composite powder particles where solid-state reactions take place. This method has several intrinsic advantages, like low temperature processing, easy control of composition, relatively inexpensive equipment, and the possibility of scaling up.

Mechanical alloying of immiscible elements leads to metastable phases and attracts considerable attention. The Fe–Cu system is regarded as a model to study the formation of phases with a positive heat of mixing. The preparation and characterization of metastable $Fe_{1-x}Cu_x$ phases has been reported by several groups [1–6]. A single-phase BCC structure is obtained for $x < 30\%$, whereas for $x > 40\%$ an FCC structure is obtained. The resulting alloy is composed of nanoparticles with a mean diameter from a few nanometres to a few tenths of a nanometre. The characterization of this system was mostly devoted to the structural, thermal and magnetic properties [1–6]. Unfortunately, still little is known about the electronic structure

0953-8984/01/245723+07$30.00

of this important model system, in particular, about the existence and nature of chemical bonding between the valence electrons. The absence of information on this important aspect of this system provided the main motivation for this study.

The purpose of this work is to study the electronic structure of a metastable $Fe_{80}Cu_{20}$ alloy. The sample was produced by ball-milling and the resulting nanoparticles had a diameter of 10 nm. The technique used in the study was core level and valence band x-ray photoelectron spectroscopy. This established technique provides useful information on the electronic structure of materials [7]. The motivation of this work is to determine the nature of the chemical bond between Fe and Cu. The core level spectra showed that the charge transfer between Fe and Cu is negligible. The valence band spectrum showed a distinct bonding interaction between the Fe 3d and Cu 3d states.

2. Experimental details

The $Fe_{80}Cu_{20}$ sample was prepared by ball-milling from a blend of Fe and Cu metal powders. The apparatus was a Spex 8000 shaker mill and the ball to powder weight ratio was 7:1. The vial was sealed in an argon atmosphere in order to prevent oxidation. The structure of the resulting powder was periodically analysed using x-ray diffraction (XRD). A single-phase (BCC) solid solution was obtained after 108 hours of milling. The diameter of the particles estimated from XRD using the Scherrer formula was 10 nm. Further details on the sample preparation and characterization will be published elsewhere.

The x-ray photoelectron spectra were taken using a commercial VG ESCA 3000 system. The base pressure in the experimental chamber was in the low 10^{-10} mbar range. The samples were cleaned by sputtering with Ar ions to remove surface contamination. The spectra were collected using Mg Kα radiation and the overall energy resolution was about 0.8 eV. The energy scale was calibrated using the Fermi level and the peak positions from the system database. The spectra were corrected by subtracting the contribution of the K$\alpha_{3,4}$ x-ray satellites. The spectra were normalized to the maximum intensity after a constant background subtraction.

3. Results and discussion

3.1. Core-level spectra

Figure 1(a) shows the Fe 2p core-level XPS spectra of pure Fe and the $Fe_{80}Cu_{20}$ alloy. The spectrum of pure Fe is in excellent agreement with previous reports [8]. The spectra are split by the 2p spin–orbit effect into the $2p_{3/2}$ and $2p_{1/2}$ regions. The spectrum of pure Fe presents a sharp $2p_{3/2}$ peak around 707.0 eV with an asymmetric tail. The tail is caused by electron–hole pair excitations in the Fe 3d open shell [9].

The Fe 2p spectrum of the $Fe_{80}Cu_{20}$ alloy is rather similar to the spectrum of pure Fe. The spectrum shows also a sharp $2p_{3/2}$ peak at 707.0 eV with the corresponding tail. The absence of chemical shift indicates that charge transfer processes are negligible. The Fe 2p spectrum of the $Fe_{80}Cu_{20}$ alloy presents a residual bump around 710.9 eV. This bump is attributed to the presence of a minority ($<3\%$) Fe_2O_3 oxide [10].

Figure 1(b) shows the Cu 2p core-level XPS spectra of the $Fe_{80}Cu_{20}$ alloy and pure Cu. The spectrum of pure Cu is in excellent agreement with previous reports [8]. The spectra are split by the 2p spin–orbit effect into the $2p_{3/2}$ and $2p_{1/2}$ regions. The spectrum of pure Cu presents a rather symmetric and sharp $2p_{3/2}$ peak around 932.7 eV. The absence of the asymmetric tail is a consequence of the Cu 3d closed shell [9].

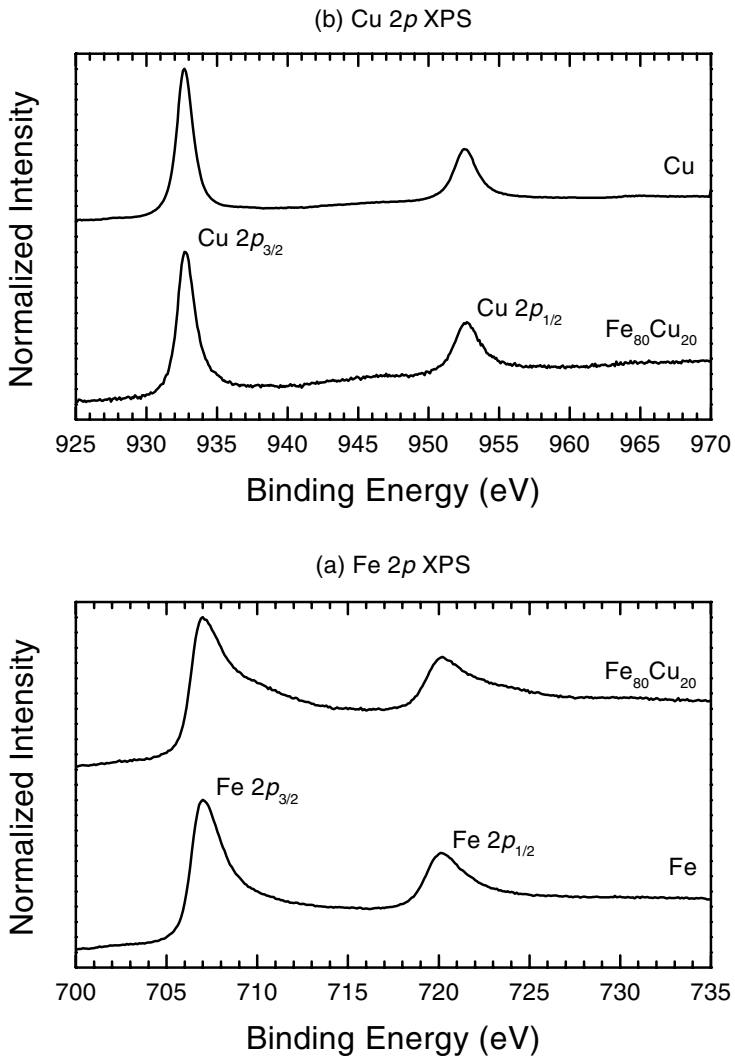

Figure 1. (a) Fe 2p core-level XPS spectra of pure Fe and the $Fe_{80}Cu_{20}$ alloy. (b) Cu 2p core-level XPS spectra of the $Fe_{80}Cu_{20}$ alloy and pure Cu.

The Cu 2p spectrum of the $Fe_{80}Cu_{20}$ alloy is strikingly similar to the spectrum of pure Cu. The spectrum shows a rather symmetric and sharp $2p_{3/2}$ peak around 932.7 eV. The absence of chemical shift indicates again that charge transfer processes are negligible. There is no evidence of a minority oxide phase in the Cu 2p spectrum of the alloy. The absence of Cu oxidation is sensible because Cu is much less reactive than Fe.

The analysis of the core-level spectra would suggest little changes at the Fe and Cu sites. The chemical shifts in the spectra are related to changes in the electrostatic potential. The absence of shifts in the spectra shows that charge transfer between Fe and Cu is negligible [7]. This precludes the partial ionic bond which is characteristic of transition metal compounds. However, there are other types of chemical bond that do not involve charge transfer processes. The valence band spectra below show evidence of bonding interactions between the Fe 3d and Cu 3d states.

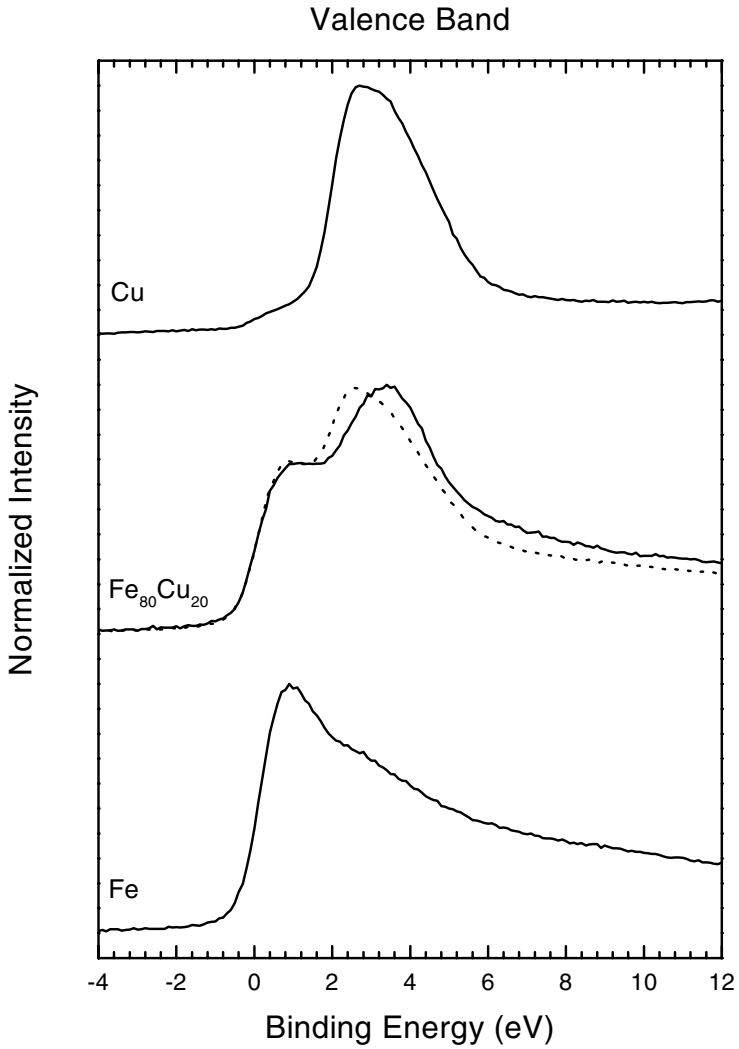

Figure 2. Valence band XPS spectra of pure Fe, the $Fe_{80}Cu_{20}$ alloy and pure Cu (solid lines), and a linear combination of the Fe and Cu spectra (dotted line).

3.2. Valence band spectra

Figure 2 shows the valence band spectra of pure Fe, the $Fe_{80}Cu_{20}$ alloy and pure Cu. These spectra are directly related to the density of states in the valence band [7]. The spectrum of Fe presents a sharp Fermi level, a strong peak at 0.9 eV, a broad shoulder around 2.9 eV and a tail towards higher binding energies. The peak and the shoulder reflect the Fe 3d density of states in the valence band. The tail corresponds to electron–hole pair excitations in the Fe 3d open shell.

The spectrum of Cu presents a weak Fermi level, a strong peak at 2.7 eV and a shoulder around 3.2 eV. The peak and the shoulder reflect the Cu 3d density of states in the valence band. The weak band extending up to the Fermi level corresponds to the Cu 4s states. The absence of the asymmetric tail is again a consequence of the Cu 3d closed shell.

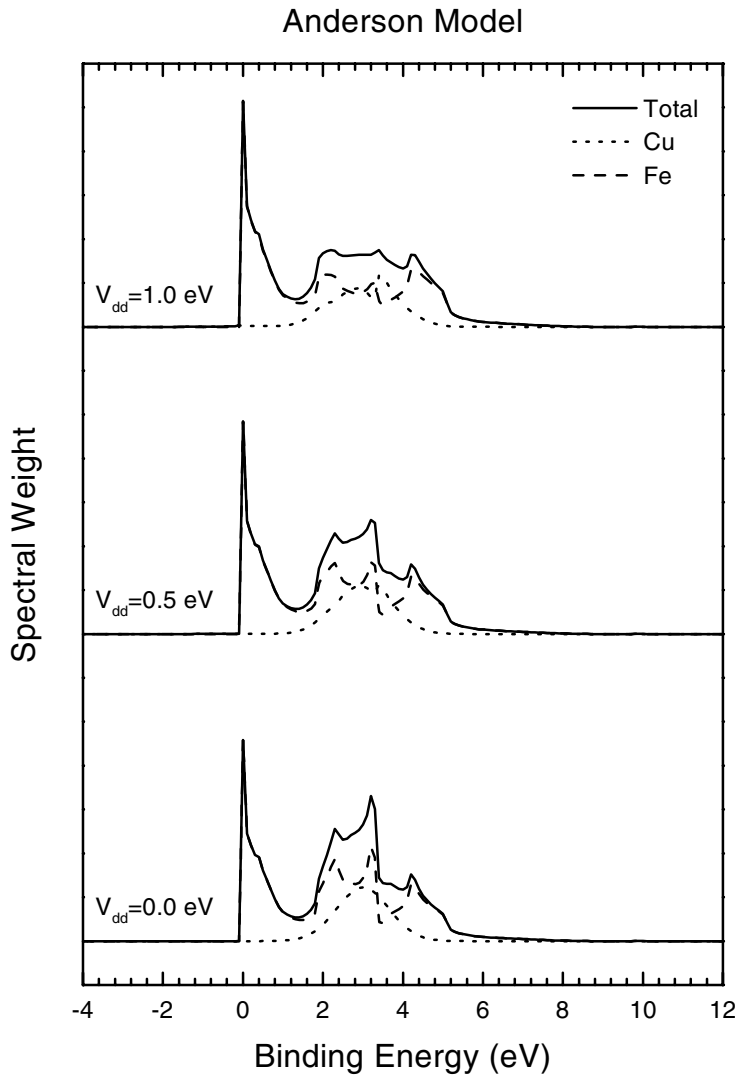

Figure 3. Generalized Anderson model calculation of the electronic structure of the $Fe_{80}Cu_{20}$ alloy as a function of the interaction parameter V_{dd}.

The spectrum of the $Fe_{80}Cu_{20}$ alloy presents a sharp Fermi level, a strong peak at 0.9 eV and a second peak at 3.5 eV. By analogy, the peak close to the Fermi level is attributed to the Fe 3d states in the alloy (the relatively weak Cu 4s band is completely masked by the stronger Fe 3d band). On the other hand, the second peak in the spectrum is attributed to the Cu 3d states in the alloy. This result is rather similar to the valence band spectra of Fe–Cu alloys obtained by sputtering [11].

The dotted line represents a weighted linear combination of the Fe and Cu spectra. The Fe 3d band region in the alloy is relatively well described by the linear combination. In contrast, the Cu 3d band region in the alloy presents clear differences with the linear combination. First, the Cu 3d band is shifted by approximately 0.6 eV towards higher binding energies. Secondly, the Cu 3d band appears narrower, more symmetric and with less structure than in pure Cu.

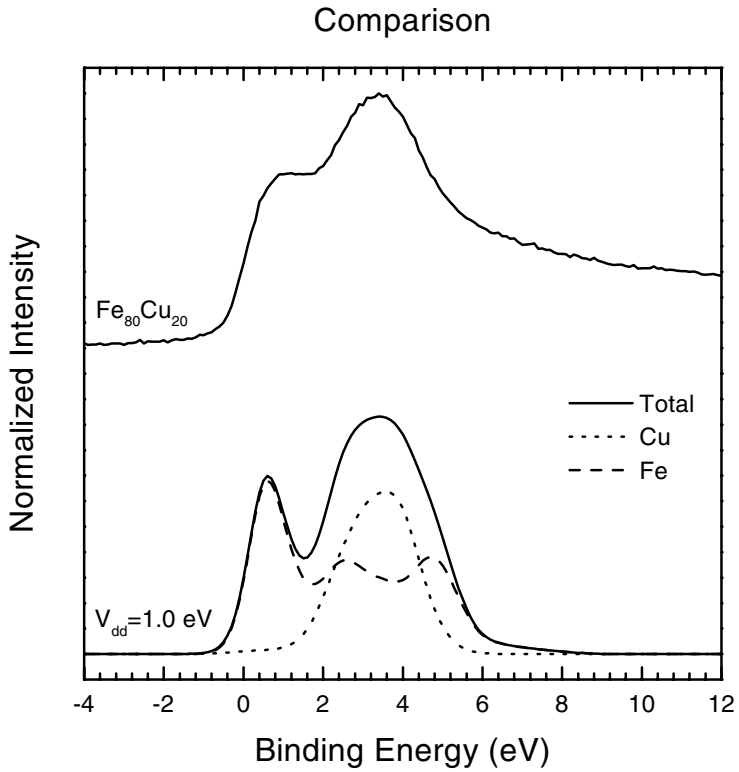

Figure 4. Comparison between the experimental valence band of $Fe_{80}Cu_{20}$ and the calculated spectrum for $V_{dd} = 1.0$ eV.

The energy shift of the Cu 3d band in the alloy is attributed to Fe 3d–Cu 3d bonding interactions. The Cu 3d band corresponds to the bonding combination with mostly Cu 3d character. Similar arguments were used in the interpretation of the valence band of Fe–Pd and Fe–Pt alloys [12]. The width of the impurity band is directly related to the DOS of the host band at the impurity level. The Cu 3d band narrowing is caused by the relatively weak Fe 3d DOS in this energy region.

3.3. Generalized Anderson model

These two effects can be understood using a generalized Anderson model calculation. This model describes reasonably well the electronic structure of concentrated alloys [13]. The starting point is the unperturbed Green function of the Fe host, denoted by g_{Fe}. The imaginary part of g_{Fe} was obtained from a compilation of LDA band structure calculations [14], whereas the real part of g_{Fe} was obtained by a Hilbert transform of the imaginary part. The unperturbed Cu impurity states, given by g_{Cu}, were simulated using a single Gaussian band. The energy position of this band was derived from the calculated Cu 3d bands of pure Cu [14]. The Fe 3d–Cu 3d interaction was introduced through the model parameter V_{dd}. The perturbed Green function of Cu, denoted by G_{Cu}, is calculated using the Dyson equation [13]

$$G_{Cu} = g_{Cu} + g_{Cu} V_{dd}^2 g_{Fe} G_{Cu}.$$

Figure 3 shows the calculated electronic structure of $Fe_{80}Cu_{20}$ as a function of V_{dd}. The Cu 3d band shifts to higher energies and broadens for increasing values of V_{dd} (the shift of the Cu 3d obtained for $V_{dd} = 1$ eV is in good agreement with the experimental result). Further, the Cu 3d band does not *resonate* with strong Fe DOS and thus remains relatively narrow. The spectral weight of the Fe 3d band is redistributed close to the Cu 3d level. However, the main Fe 3d states close to the Fermi level remain relatively unchanged. All these effects resemble very closely those observed in the experimental spectrum. In addition, these results are in good agreement with LMTO-CPA calculations for the Fe–Cu system [15].

Figure 4 shows a comparison of the $Fe_{80}Cu_{20}$ valence band with the calculated spectrum for $V_{dd} = 1$ eV. The calculation was broadened with a 0.8 eV Gaussian to simulate the experimental resolution. The spectral weight was also normalized to take into account the relative photoemission cross sections. The calculation reproduces reasonably well the energy position and width of the Cu 3d band. The calculated spectrum does not include dynamic effects like electron–hole pair creation. Consequently, the calculation does not reproduce the asymmetric tail in the experimental spectrum.

The samples used in this study were produced *ex situ* and then cleaned by sputtering in the apparatus. In principle, this could induce secondary processes such as surface segregation, point defects etc. We think that the main conclusions drawn here are not critically affected by such processes.

4. Summary and conclusions

In summary, we studied the electronic structure of a metastable $Fe_{80}Cu_{20}$ alloy. The sample was produced by ball-milling and the nanoparticles had around 10 nm. The technique used in the study was core-level and valence band XPS. The core-level spectra show that the charge-transfer between Fe and Cu is negligible. The valence band spectra reflect the bonding between the Fe 3d and Cu 3d states. This illustrates chemical bonding in a metastable alloy of immiscible elements.

Acknowledgments

This work was partially supported by the Brazilian Funding Agencies CNPq, CAPES, Finep and Pronex.

References

[1] Uenishi K, Kobayashi K F, Nasu S, Hatano H, Ishihara K N and Shingu P H 1992 *Z. Metallkd.* **83** 132
[2] Yavari A R, Desre P J and Benameur T 1992 *Phys. Rev. Lett.* **68** 2235
[3] Jiang J Z, Gonser U, Gente C and Bormann R 1993 *Appl. Phys. Lett.* **63** 1056
[4] Crespo P, Hernando A, Yavari R, Drbohlav O, Escorial A G, Barandiaran J M and Orue I 1993 *Phys. Rev.* B **48** 7134
[5] Macri P P, Rose P, Frattini R, Enzo S, Principi G, Hu W X and Cowlan N 1994 *J. Appl. Phys.* **76** 4061
[6] Schilling P J, He J H, Cheng J and Ma E 1996 *Appl. Phys. Lett.* **68** 767
[7] Hüfner S 1995 *Photoelectron Spectroscopy* (Berlin: Springer)
[8] Moulder J F, Stickle W F, Sobol P E and Bomben K 1995 *Handbook of X-Ray Photoelectron Spectroscopy* (Eden Prairie: Perkin-Elmer)
[9] Abbate M 1989 *Phys. Rev.* B **39** 7641
[10] Pereira C A M, Abbate M, Schreiner W H, Boff M A S and Teixeira S R 2000 *Solid State Commun.* **116** 457
[11] Uchida M, Tanaka K, Sumiyama K and Makamura Y 1989 *J. Phys. Soc. Japan* **58** 1725
[12] van Acker J F, Weijs P J W, Fuggle J C, Horn K and Buschow K H J 1991 *Phys. Rev.* B **43** 8903
[13] van Acker J F, Lindeyer E W and Fuggle J C 1991 *J. Phys.: Condens. Matter* **3** 9579
[14] Moruzzi V L, Janak J F and Williams A R 1978 *Calculated Electronic Properties of Metals* (Oxford: Pergamon)
[15] Kudrnovsky J, Bose S K and Andersen O K 1990 *J. Phys. Soc. Japan* **59** 4511